Androgen-dependent pathology demonstrates myopathic contribution to the Kennedy disease phenotype in a mouse knock-in model

Zhigang Yu,[1] Nahid Dadgar,[1] Megan Albertelli,[2] Kirsten Gruis,[3] Cynthia Jordan,[4] Diane M. Robins,[2] and Andrew P. Lieberman[1]

[1]Department of Pathology, [2]Department of Human Genetics, and [3]Department of Neurology, University of Michigan Medical School, Ann Arbor, Michigan, USA. [4]Department of Psychology and Neuroscience Program, Michigan State University, East Lansing, Michigan, USA.

Kennedy disease, a degenerative disorder characterized by androgen-dependent neuromuscular weakness, is caused by a CAG/glutamine tract expansion in the *androgen receptor* (*Ar*) gene. We developed a mouse model of Kennedy disease, using gene targeting to convert mouse androgen receptor (AR) to human sequence while introducing 113 glutamines. AR113Q mice developed hormone and glutamine length–dependent neuromuscular weakness characterized by the early occurrence of myopathic and neurogenic skeletal muscle pathology and by the late development of neuronal intranuclear inclusions in spinal neurons. AR113Q males unexpectedly died at 2–4 months. We show that this androgen-dependent death reflects decreased expression of skeletal muscle chloride channel 1 (CLCN1) and the skeletal muscle sodium channel α-subunit, resulting in myotonic discharges in skeletal muscle of the lower urinary tract. AR113Q limb muscles show similar myopathic features and express decreased levels of mRNAs encoding neurotrophin-4 and glial cell line–derived neurotrophic factor. These data define an important myopathic contribution to the Kennedy disease phenotype and suggest a role for muscle in non–cell autonomous toxicity of lower motor neurons.

Introduction

Kennedy disease, or spinal and bulbar muscular atrophy, is one of 9 neurodegenerative disorders that result from the expansion of CAG/glutamine tracts in the coding regions of otherwise unrelated genes (1). In Kennedy disease, an expanded glutamine tract near the amino terminus of the androgen receptor (AR) leads to hormone-dependent protein misfolding and to the predominant loss of lower motor neurons in the brainstem and spinal cord of affected males (2). Clinical onset occurs during adolescence or adulthood and is characterized initially by muscle cramps and elevated serum creatine kinase (3, 4). These myopathic features commonly precede muscle weakness, which inevitably develops as the disease progresses and is most severe in the proximal limb and bulbar muscles. As with all of the polyglutamine disorders, the mechanisms that lead to selective neuronal dysfunction and degeneration are poorly understood.

In Kennedy disease, several general principles have emerged that guide our understanding of disease pathogenesis. Amino-terminal fragments of the AR exhibit glutamine length–dependent toxicity in both cell-based and animal models (5, 6). This toxicity is accompanied by activation of the unfolded protein response (7), disruption of intracellular transport (8–10), and evidence of transcriptional dysregulation (11, 12). Model systems using the full-length AR protein establish that the AR's toxicity is dependent on the presence of androgen (13–16) and is regulated, in part, by hormone-dependent retrograde transport (17, 18). This ligand dependence of the disease phenotype provides a mechanistic explanation for the minimal effects of the mutant *Ar* allele in females (19, 20) and offers an important therapeutic approach for treating men with this disorder (14, 21).

Studies in several cell-based model systems have also indicated that the AR undergoes a partial loss of normal function as the glutamine tract expands (22–25). Patients with Kennedy disease exhibit signs of partial androgen insensitivity, including testicular atrophy and decreased fertility (26). Since androgens exert trophic effects on lower motor neurons, this led to speculation that partial loss of normal AR function contributes to the selective neuronal vulnerability.

In order to study disease pathogenesis, we generated a mouse model of Kennedy disease that reproduces both the hormone-dependent neuromuscular weakness and the systemic pathology by which this disorder is characterized. Using gene targeting, we exchanged 1340 bp of coding sequence from mouse *Ar* exon 1 with human exon 1 and in the process inserted 21, 48, or 113 CAG repeats (27, 28). The targeted *Ar* allele encodes a protein that is identical to human AR except at 4 amino acids encoded by exon 1 and a few in the hinge domain that differ between humans and mice. This receptor is expressed at endogenous levels through control of mouse *Ar* gene regulatory elements. Mice with the targeted insertion of 21 or 48 CAG repeats (AR21Q and AR48Q, respectively) are similar to WT while those with an insertion of 113 CAG repeats (AR113Q) model the systemic manifestations of Kennedy disease. AR113Q mice exhibit testicular atrophy and decreased fertility due to toxicity of the mutant protein, resulting in abnormalities of germ cell maturation and the Sertoli cell

Nonstandard abbreviations used: AR, androgen receptor; CLCN1, chloride channel 1; GDNF, glial cell line–derived neurotrophic factor; MyoD, myogenic differentiation antigen; NT-4, neurotrophin-4; rRNA, ribosomal RNA; SCN4A, voltage-gated sodium channel, α-subunit; SOD1, Cu/Zn superoxide dismutase.

Conflict of interest: The authors have declared that no conflict of interest exists.

Citation for this article: *J. Clin. Invest.* **116**:2663–2672 (2006). doi:10.1172/JCI28773.

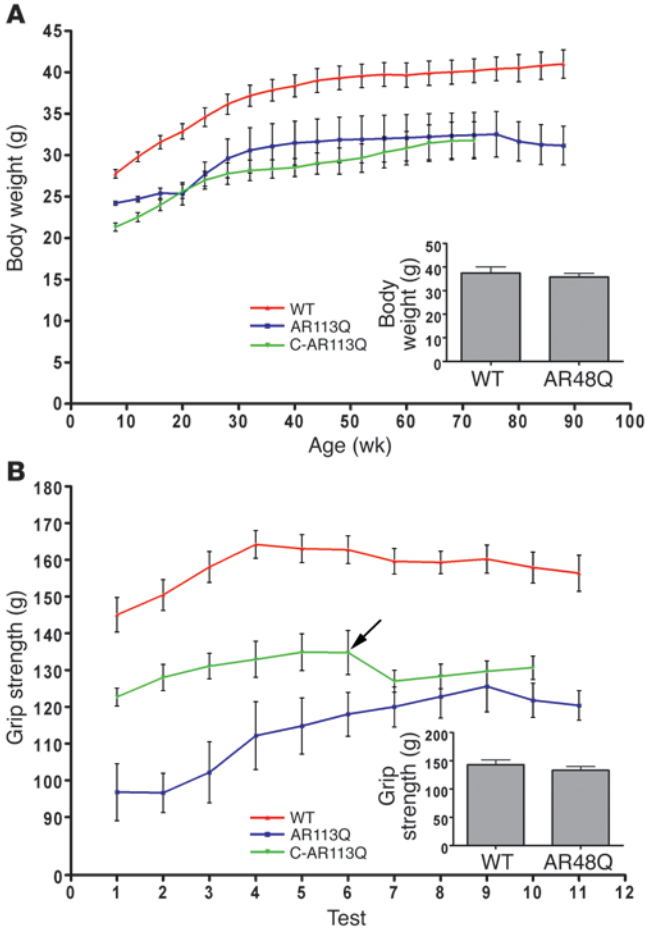

Figure 1
AR113Q males are smaller and weaker than WT littermates. (**A**) Body mass (mean ± SD) reported by age of WT (red line, $n = 9$), AR113Q (blue line, $n = 5$–22 depending on age, due to early death), and castrated AR113Q males (C-AR113Q) (green line, $n = 9$). AR113Q males were significantly smaller than WT ($P < 0.001$), and castration further decreased body mass ($P < 0.05$ by ANOVA with the Neuman-Keuls multiple comparison test). Inset shows body mass of AR48Q ($n = 7$) and WT ($n = 5$) males at 22–23 months ($P > 0.05$ by unpaired Student's t test). (**B**) Forelimb grip strength (mean ± SD) of WT (red line, $n = 13$), AR113Q (blue line, $n = 5$), and castrated AR113Q males (green line, $n = 9$) evaluated monthly beginning at 11–13 months. The 3 curves are significantly different from each other ($P < 0.001$ by ANOVA with the Neuman-Keuls multiple comparison test). Implantation of testosterone pellets into castrated AR113Q males at 17–19 months is indicated by arrow. Inset shows grip strength of AR48Q ($n = 7$) and WT ($n = 5$) males at 22–23 months ($P > 0.05$ by unpaired Student's t test).

cytoskeleton that are distinct from changes caused by an *Ar*-null mutation (27). These data indicate that aspects of Kennedy disease phenotype previously attributed to a partial loss of AR function are in actuality mediated by toxicity conferred by the expanded glutamine tract.

Here we characterize the neuromuscular phenotype of AR113Q mice. Mutant males exhibit androgen-dependent neuromuscular weakness. Skeletal muscle pathology precedes pathologic changes in spinal cord, shows evidence of both myopathic effects and neurogenic atrophy mediated by the expanded glutamine AR, and reproduces the mixed features previously described in Kennedy disease muscle (29, 30). AR113Q males unexpectedly die at a young age, and our analyses implicate altered muscle membrane excitability in the pathogenesis. These data define an important myopathic contribution to the disease and suggest a role for muscle in non–cell autonomous neuronal dysfunction.

Results

Androgen-dependent neuromuscular weakness in AR113Q mice. Mice with a targeted insertion of 113 CAG repeats into exon 1 of the *Ar* gene were examined for evidence of an androgen-dependent neuromuscular phenotype. Since the *Ar* gene is on the X chromosome, males are hemizygous for either the mutant or WT allele, allowing for ready comparison of littermates. Body mass of AR113Q males was significantly less than that of WT males at all ages examined (Figure 1A). In contrast, male mice with a targeted *Ar* allele containing 48 CAG repeats were of normal size (Figure 1A). Surgical castration of AR113Q males at 4–5 weeks of age, just prior to the onset of puberty, caused a slight further decrease in mean body mass. To measure skeletal muscle strength, we performed forelimb grip-strength analyses on WT, AR113Q, and castrated AR113Q males (Figure 1B). AR113Q males had significantly decreased forelimb strength compared with WT littermates. This deficit appeared in adults as early as 8 weeks of age (138 g ± 5.2 g for WT [$n = 14$] versus 103 g ± 4.9 g for AR113Q [$n = 8$]; $P = 0.0002$). That this decreased strength was glutamine length–dependent was confirmed by grip-strength analyses on 22- to 23-month-old AR48Q males, which had forelimb strength similar to that of WT mice (Figure 1B). Surgical castration partially rescued the grip-strength deficit in AR113Q males, suggesting that this weakness was androgen dependent. To confirm this and to exclude possible developmental effects, we implanted testosterone pellets subcutaneously into castrated AR113Q males at 17–19 months of age (Figure 1B). Testosterone-treated, castrated AR113Q males exhibited forelimb grip strength similar to that of noncastrated AR113Q males and no longer showed partial rescue of the phenotype. These data establish that AR113Q males exhibit androgen-dependent deficits of forelimb grip strength that model skeletal muscle weakness of males with Kennedy disease.

This functional deficit on behavioral testing of AR113Q males was accompanied by morphologic changes in skeletal muscle indicative of both neurogenic and myopathic effects, similar to the mixed features described in biopsies of Kennedy disease muscle (29, 30). Hind-limb muscle of AR113Q males contained groups of angulated, atrophic fibers suggestive of neurogenic atrophy (Figure 2A). Also present were large, rounded fibers with internal nuclei, indicative of a myopathic process (Figure 2A). AR immunoreactive intranuclear inclusions were identified in muscle fibers of AR113Q males (Figure 2A) as young as 10–15 weeks, increased in frequency with age, and by 20 weeks also stained for ubiquitin (Figure 2A). In contrast, no changes were observed in skeletal muscle of WT or AR48Q males (not shown).

To determine whether changes in gene expression reflective of denervation occurred in AR113Q muscle, quantitative real-time RT-PCR was used to measure levels of *myogenin*, *acetylcholine receptor α-subunit*, and *myogenic differentiation antigen* (*MyoD*) mRNAs. These transcripts are induced following denervation (31–33) but not in skeletal muscle from mouse models or patients with Hun-

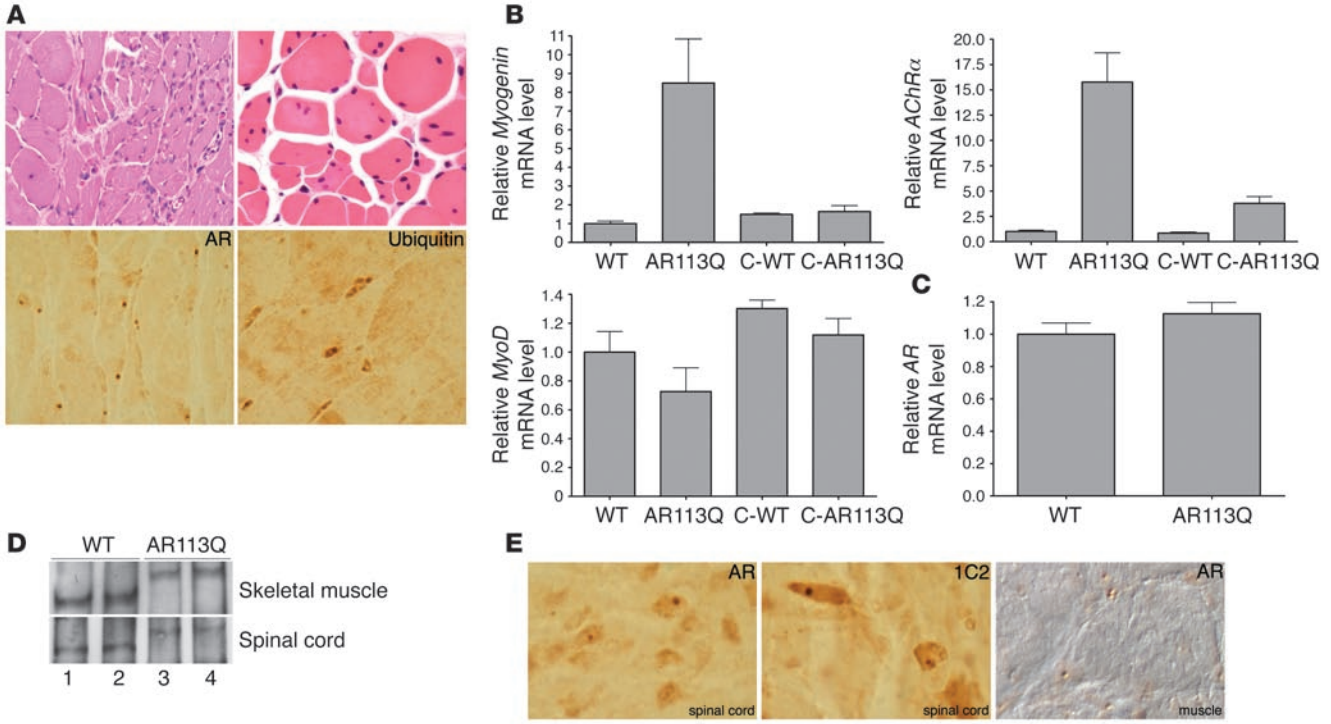

Figure 2

Neuromuscular pathology in AR113Q male mice. (**A**) Grouped atrophic, angulated fibers (upper left) and marked variation in fiber size and internally placed nuclei (upper right) are present in hind-limb skeletal muscle of AR113Q males. Magnification, ×400 (upper left); ×1000 (upper right). AR (lower left) and ubiquitin (lower right) immunoreactive intranuclear inclusions are also present. Magnification, ×1000. (**B**) Relative *myogenin*, *acetylcholine receptor α-subunit* (*AChRα*), and *MyoD* mRNA expression levels in hind-limb muscle as determined by quantitative real-time RT-PCR. Data are from WT (n = 8), AR113 (n = 8), and castrated WT males (C-WT) (n = 6) at 3–5 months and castrated AR113Q males at 18 months (n = 4). Results are reported as mean ± SD relative to expression of 18s rRNA. Expression levels of myogenin and acetylcholine receptor α-subunit mRNA in AR113Q muscle are significantly different from those in all other groups ($P < 0.01$ and $P < 0.001$, respectively, by ANOVA with the Neuman-Keuls multiple comparison test). Expression of *MyoD* mRNA in AR113Q and WT muscle is not significantly different. (**C**) Relative *AR* mRNA expression levels in hind-limb muscle of WT (n = 8) and AR113Q males (n = 8) at 3–5 months ($P > 0.05$). (**D**) AR protein expression in skeletal muscle (top panel) and spinal cord (bottom panel) of WT (lanes 1 and 2) and AR113Q males (lanes 3 and 4) at 3–4 months detected by immunoprecipitation and Western blot. (**E**) Intranuclear inclusions in spinal cord and skeletal muscle of AR113Q mice at 24 months detected by immunohistochemistry for AR and expanded glutamine tract (1C2). Magnification, ×1000.

tington disease (34), another polyglutamine expansion disorder. AR113Q skeletal muscle expressed 8- to 15-fold higher levels of *myogenin* and *acetylcholine receptor α-subunit* mRNAs compared with WT muscle (Figure 2B) whereas expression of *MyoD* mRNA was not significantly changed. Surgical castration of AR113Q males restored expression of *myogenin* and *acetylcholine receptor α-subunit* mRNAs toward WT levels, demonstrating that these differences in gene expression are androgen dependent.

To further establish the relationship between skeletal muscle and spinal cord pathology, we evaluated AR expression in young and old WT and mutant males. Quantitative real-time RT-PCR demonstrated that *AR* mRNA levels were equivalent in hind-limb skeletal muscle of WT and mutant males at 3–5 months (Figure 2C). Soluble protein detectable by immunoprecipitation was slightly decreased in skeletal muscle and spinal cord of mutant males (Figure 2D), likely reflecting the formation of insoluble protein complexes by the expanded glutamine receptor, similar to those previously detected in other tissues (27). Despite the appearance of frequent AR intranuclear inclusions in muscle of 3- to 5-month-old mutant males, no spinal cord pathology was detected in animals at this age (not shown). Neuronal intranuclear inclusions were detectable in spinal cord of AR113Q males only at 24 months (Figure 2E), a time point when hind-limb skeletal muscle also contained frequent intranuclear aggregates. Sections of brain, liver, and kidney from these aged AR113Q males were also surveyed for AR intranuclear inclusions, and none were identified (not shown).

Androgen-dependent early death in AR113Q males. Analysis of life span revealed that AR113Q males died at a young age. As shown in Figure 3A, approximately 80% of AR113Q males died between 8 and 20 weeks while none of the WT males or heterozygous mutant females (Figure 4E) died in this same period. Early death was glutamine-length dependent, as all 6 AR21Q and 9 AR48Q males aged to 24 months survived (not shown). Three lines of evidence confirmed that early death was due to the expanded glutamine AR and not another factor, such as a secondary mutation generated during gene targeting. First, the phenotype was unchanged as mice were backcrossed to C57BL/6J. The survival curve of second-generation backcrossed AR113Q (N2 AR113Q) males (Figure 3A) was not significantly different from that of N5 AR113Q males (Figure 3B). Second, an additional line of AR113Q mice was established from an independently targeted

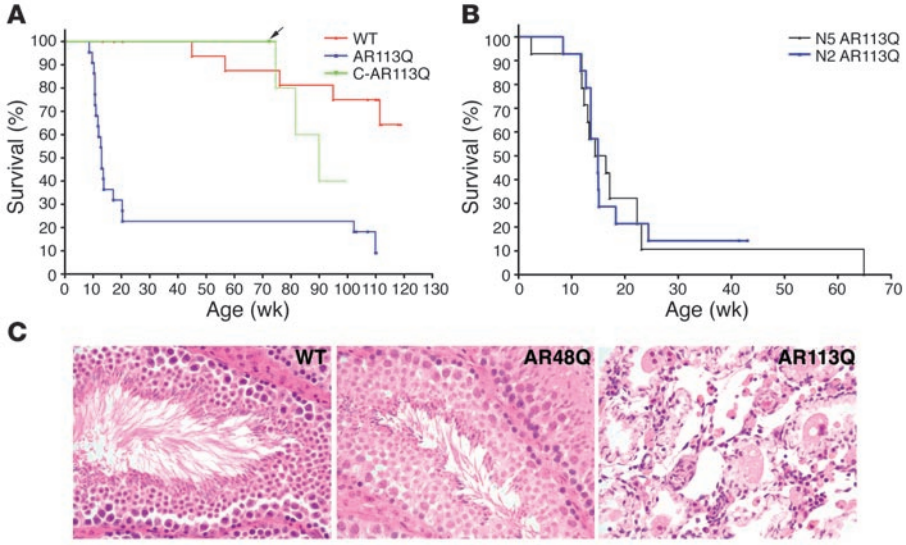

Figure 3
Early death in AR113Q males is androgen dependent. (**A**) Survival curve of littermate N2 WT (red line, $n = 19$), AR113Q (blue line, $n = 22$), and castrated AR113Q males (green line, $n = 9$). Four of the castrated AR113Q males were euthanized at 18 months (indicated by arrow), and the remaining 5 were implanted with testosterone pellets and monitored for survival. (**B**) Survival curve of N5 AR113Q males from the original line (black line, $n = 14$) and N2 AR113Q males from an independently generated second line (blue line, $n = 14$). (**C**) Testes of WT, AR48Q, and AR113Q males at 24 months. Magnification, ×400.

ES cell clone and exhibited this same phenotype, with superimposable survival curves (Figure 3B). Third, surgical castration completely prevented early death (Figure 3A). All N2 mutant males that were castrated at 5 weeks survived for 18 months, establishing that early death was androgen dependent. In support of this conclusion was the fact that testosterone pellet implantation in aged, castrated AR113Q males resulted in death of 60% of mice within 6 months, during which time only approximately 20% of WT males died (Figure 3A).

Although many AR113Q males died by 20 weeks, approximately 10%–20% survived significantly longer. The basis for the survival of this subset of mice is unknown, and longer life spans did not correlate with lower serum testosterone levels at 10–12 weeks of age (data not shown). However, mutant males that survived to 8–10 months had uniformly low serum testosterone levels. These levels contrasted with the wide range of serum testosterone measured in WT mice (0.64 ± 0.07 ng/ml in AR113Q versus 3.2 ± 1.45 ng/ml in WT). When euthanized at 24 months, AR113Q males were found to have markedly atrophic testes that showed a complete loss of normal cellular elements within the seminiferous tubules (Figure 3C). This pathology reflects an age-dependent progression of the defects in Sertoli and germ cells previously described in AR113Q mice (27) and contrasts with the normal appearance of testes from comparably aged WT and AR48Q males. We conclude that early death of AR113Q males depended upon circulating testosterone. Animals that survived past 20 weeks were protected from death by progressive testicular atrophy that resulted in impaired testosterone production.

Early death was observed in AR113Q males and not females. To determine whether this was due to differences in androgen levels, we implanted testosterone or control pellets into AR113Q heterozygous

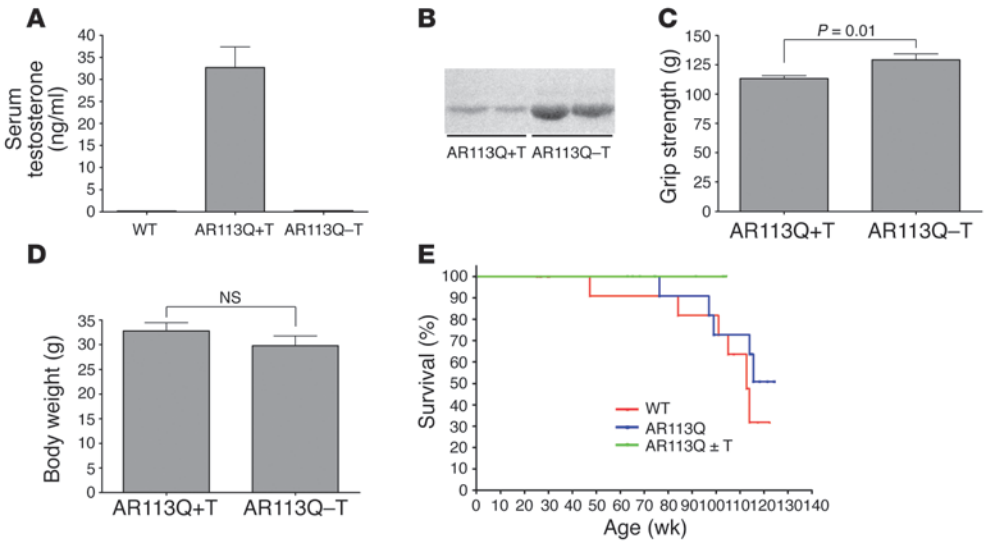

Figure 4
Testosterone-treated AR113Q females exhibit normal life span. (**A**–**D**) Testosterone-dependent effects on heterozygous AR113Q females. AR113Q females were implanted with testosterone (+T, $n = 8$) or vehicle control (–T, $n = 7$) pellets at 2–4 months. Serum testosterone levels, determined at 4–7 months, were significantly increased in hormone-treated mice compared with controls ($P < 0.001$) (**A**). Excretion of major urinary proteins (**B**) was compared in AR113Q–T and AR113Q+T females. AR113Q+T females showed a small but significant deficit in forelimb grip strength (**C**) ($P = 0.01$ by unpaired Student's t test) but unchanged body mass (**D**) ($P = 0.3$ by unpaired Student's t test) compared with AR113Q–T females at 16 months. (**E**) Survival curves of AR113Q+T ($n = 8$) and AR113Q–T ($n = 7$) (overlapping green lines), untreated AR113Q females (blue line, $n = 11$), and WT females (red line, $n = 19$) were similar ($P > 0.05$). None of the AR113Q+T or AR113Q–T females died during the study; half were euthanized at 16–19 months, and the remainder were euthanized at 23–26 months.

Table 1
Moribund AR113Q males are azotemic and hyperkalemic

	Blood urea nitrogen (mg/dl)	Creatinine (mg/dl)	Na^+ (mM)	K^+ (mM)	Cl^- (mM)
Reference range	18.0–29.0	0.20–0.80	126.0–182.0	4.70–6.40	92.0–120.0
Animal 1	284.4	1.90	148.9	Out of linear range	112.3
Animal 2	> 130.0	1.57	171.6	7.99	122.0
Animal 3	> 130.0	1.17	157.2	9.89	122.9
Animal 4	> 260	1.87	146.0	Sample hemolyzed	110.9

females at 2–4 months. Testosterone-treated AR113Q females had elevated serum testosterone levels (Figure 4A). To confirm that these animals responded to hormone treatment, we evaluated expression of an androgen-regulated gene. Testosterone-treated AR113Q females excreted elevated levels of major urinary proteins (Figure 4B), pheromone-binding proteins whose expression is under indirect regulation by androgens (35). Testosterone-treated AR113Q females also developed small but statistically significant deficits in forelimb grip strength (Figure 4C) without altered body mass (Figure 4D). However, testosterone-treated AR113Q females had survival rates similar to those of vehicle-treated AR113Q females and WT females (Figure 4E). These data establish that AR113Q females develop androgen-dependent weakness but do not exhibit the early death manifested by AR113Q males.

Myopathic contribution to disease phenotype. We next sought to determine the mechanism leading to death of AR113Q males. Although many mutant males suddenly became moribund and rapidly died, we were able to collect serum from 4 animals before death. Evaluation of serum electrolytes, blood urea nitrogen, and creatinine revealed changes consistent with acute urinary tract obstruction (markedly elevated blood urea nitrogen, creatinine, and potassium; normal sodium and chloride; see Table 1). These abnormalities of blood chemistry and the repeated observation at necropsy of markedly distended bladders without evidence of physical obstruction prompted us to explore the neuromuscular system of the lower urinary tract. We studied the spinal nucleus of the bulbocavernosus and the levator ani/bulbocavernosus muscles as one component of this system. This neuromuscular circuit persists in male rodents but not in females and mediates normal copulatory behavior (36). Both the lower motor neurons of this system and the skeletal muscles they innervate express high levels of AR protein and require androgens for their survival and proper function (36–42).

Examination of the levator ani/bulbocavernosus muscles from AR113Q males as young as 3 months revealed atrophic fibers with frequent internal nuclei and prominent AR intranuclear inclusions (Figure 5A). AR intranuclear inclusions were also present in muscles of castrated AR113Q males, indicating that their occurrence was not hormone dependent and did not correlate with early death. Muscles from WT and AR48Q mice were devoid of morphologic changes (not shown). Quantitative real-time RT-PCR demonstrated significant elevations of *myogenin* and *acetylcholine receptor α-subunit* mRNAs in AR113Q levator ani/bulbocavernosus muscles while *MyoD* mRNA expression was not statistically different from that of WT (Figure 5B). These morphologic and gene expression changes were similar to those observed in hind-limb muscle (Figure 2, A and B) and were consistent with mixed pathology mediated by denervation and myopathy. The effects of surgical castration on gene expression in the levator ani/bulbocavernosus muscles were complex and likely reflected the exquisite sensitivity of both the muscles and innervating motor neurons to androgens. Surgical castration did not significantly decrease expression of *myogenin* and *acetylcholine receptor α-subunit* mRNAs in AR113Q males and significantly increased the expression levels of *MyoD* and myogenin mRNAs in WT males (Figure 5B). These data are consistent with the notion that androgens regulate the expression of these mRNAs through either direct effects on the levator ani/bulbocavernosus muscles or indirect effects on their innervating motor neurons.

We next considered the possibility that altered excitability of skeletal muscles in the lower urinary tract might contribute to urinary tract obstruction in AR113Q males. We examined 2 possible mediators of this effect, the skeletal muscle chloride channel 1 (CLCN1) and the skeletal muscle *voltage-gated sodium channel type IV, α-subunit* (*Scn4a*). Denervation is known to decrease expression of CLCN1 in skeletal muscle (31). Muscle membrane excitability is affected by changes in CLCN1 expression, as evidenced by mutations in the encoding *Clcn1* gene in patients with myotonia congenita (43) and by decreased expression of CLCN1 protein in humans and mouse models of myotonic dystrophy (44–46). Similarly, mutations in *Scn4a* cause paramyotonia congenita, hyperkalemic periodic paralysis, and potassium-aggravated myotonia in humans (47). These mutations result in gain-of-function defects whereby channels pass more sodium current than normal.

Indirect immunofluorescence revealed a loss of CLCN1 protein expression in levator ani/bulbocavernosus muscles of AR113Q males (Figure 6A). Surgical castration, which prevented early death of AR113Q males, restored CLCN1 expression. In contrast to the levator ani/bulbocavernosus muscles, hind-limb skeletal muscle of AR113Q males expressed readily detectable levels of CLCN1 protein.

Decreased CLCN1 protein expression resulted from lower levels of *CLCN1* mRNA. Quantitative real-time RT-PCR showed that mRNA levels in the levator ani/bulbocavernosus muscles of AR113Q males were decreased to approximately 25% of that of WT males and that this deficit was partially corrected by surgical castration (Figure 6B). No evidence of aberrant mRNA splicing of exons 7a and 8a was obtained (not shown). Similar changes in *CLCN1* mRNA accumulation were also observed in AR113Q hind-limb muscle (Figure 6C). Continued expression of CLCN1 protein in this muscle likely reflects that limb muscles showed a less severe decrease in *CLCN1* mRNA accumulation than did levator ani/bulbocavernosus muscles. Additional effects on processes that regulate the channel's expression in levator ani/bulbocavernosus muscles, such as translation and trafficking to the plasma membrane, cannot be excluded.

Similar androgen-dependent effects on *SCN4A* mRNA expression were demonstrated in levator ani/bulbocavernosus muscles of AR113Q males (Figure 6D). In contrast, AR113Q hind-limb muscle expressed *SCN4A* mRNA at WT levels (Figure 6E). Indirect immunofluorescence revealed sodium channel expression patterns in levator ani/bulbocavernosus and hind-limb muscles that were similar to those observed for CLCN1 and that paralleled changes in *SCN4A* mRNA expression (not shown).

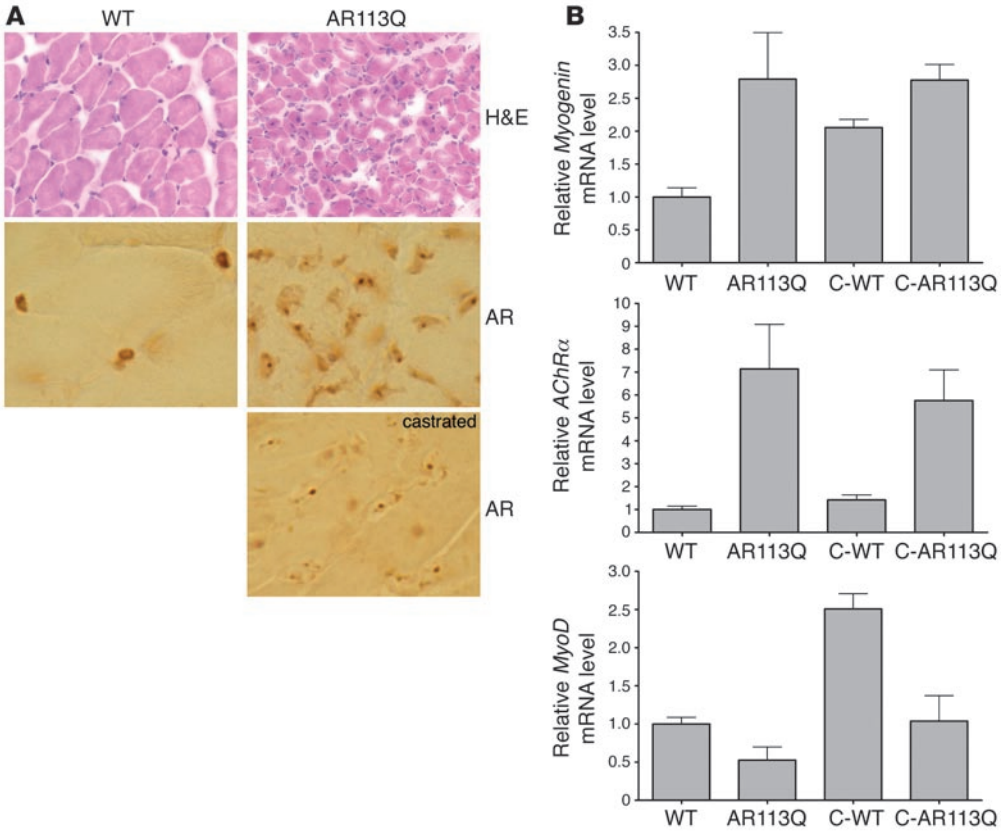

Figure 5
Levator ani/bulbocavernosus muscles exhibit severe pathology in young AR113Q males. (**A**) Representative images of levator ani/bulbocavernosus muscle from WT and AR113Q males. Magnification, ×400 (top row). Frequent AR immunoreactive intranuclear inclusions were present in muscle from AR113Q but not WT mice. Magnification, ×1000 (middle row). Muscle from castrated AR113Q males also contained frequent AR immunoreactive intranuclear inclusions. Magnification, ×1000 (bottom row). (**B**) Altered expression of *myogenin* and *acetylcholine receptor α-subunit* mRNA but not *MyoD* mRNA in AR113Q muscle. Relative mRNA expression levels were determined by quantitative real-time RT-PCR. Data are from WT ($n = 7$), AR113Q ($n = 8$), and castrated WT males ($n = 6$) at 3–5 months and surgically castrated AR113Q males at 18 months ($n = 4$). Results are reported as mean ± SD relative to expression of 18s rRNA. Differences between WT and AR113Q are significant at $P < 0.05$ for myogenin and acetylcholine receptor α-subunit mRNA by ANOVA with the Neuman-Keuls multiple comparison test. Expression of MyoD mRNA is not different between WT and AR113Q.

To determine whether AR113Q skeletal muscle exhibited altered electrical excitability, we performed needle electromyography on hind-limb and levator ani/bulbocavernosus muscles (Figure 7A). All AR113Q males examined had abnormal electrical activity triggered by needle insertion, consisting of positive waves oscillating in amplitude for more than 300 ms, characteristic of myotonic discharges. Abnormal insertional activity was seen more frequently in the levator ani/bulbocavernosus muscles than in the hind-limb muscles of AR113Q males and was not recorded in either muscle group of WT males. Additionally, abnormal spontaneous activity indicative of denervation was recorded in all AR113Q males in both the levator ani/bulbocavernosus and hind-limb muscles (Figure 7A). Abnormal spontaneous activity consisted of sustained and unsustained regularly firing positive waves that occurred at a low frequency (<30 Hz). Abnormal spontaneous activity was seen more frequently in levator ani/bulbocavernosus muscles (approximately 50% of needle insertions) than in hind-limb muscles (approximately 25% of needle insertions). No abnormal spontaneous activity was detected in WT mice. Thus, needle electromyography demonstrated electrical activity in AR113Q skeletal muscle indicative of both myopathic and neurogenic processes.

Finally, to begin to explore whether myopathic effects could contribute more broadly to the Kennedy disease phenotype, we examined the expression of trophic factors in muscle that are known to influence motor neuron survival (48). We found that hind-limb muscle from AR113Q males expressed significantly lower levels of *neurotrophin-4* (*NT-4*) and *glial cell line–derived neurotrophic factor* (*GDNF*) mRNAs than did WT muscle (Figure 7B). A similar trend was observed for the expression of *IGF-1* mRNA although differences did not reach statistical significance (not shown). Surgical castration restored the expression of *NT-4* but not *GDNF* mRNA to WT levels. These data suggest that myopathic effects mediated by the expanded glutamine AR may influence motor neuron survival by altering the expression of muscle-derived neurotrophic factors.

Discussion

We have used gene targeting to develop a knock-in mouse model of Kennedy disease. These mice express a humanized form of AR in which much of the coding region of mouse exon 1 is exchanged for human sequence. Expression of the targeted *Ar* gene is under the control of the endogenous mouse regulatory elements, resulting in expression patterns that are similar to that of the WT allele. Mice containing the targeted *Ar* allele encoding glutamine tracts of 21 or 48 residues phenotypically resemble WT while those expressing 113 glutamines model the systemic and neuromuscular features of Kennedy disease. AR113Q knock-in males exhibit testicular atrophy and decreased fertility that are a manifestation of the toxicity conferred by the expanded glutamine tract (27). Here we demonstrate that these mice also develop androgen-dependent neuromuscular weakness that is reminiscent of the phenotype manifested by Kennedy disease patients.

Hind-limb skeletal muscle of AR113Q males exhibited morphologic and gene expression changes indicative of both neurogenic and myopathic effects, similar to the mixed features described in Kennedy disease muscle (29, 30). Muscle pathology, including morphological changes in myofibers, as well as AR and ubiquitin

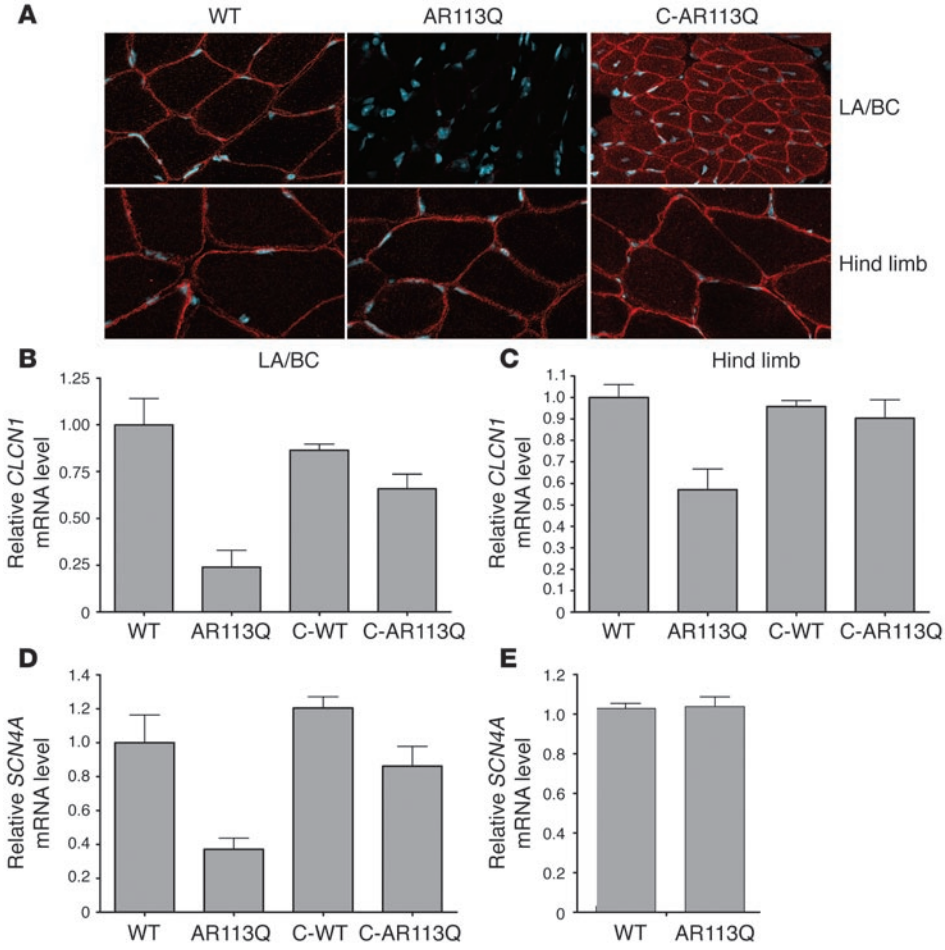

Figure 6
Androgen-dependent decrease of CLCN1 and SCN4A expression in AR113Q skeletal muscle. (**A**) Indirect immunofluorescence demonstrates CLCN1 protein expression (red) in levator ani/bulbocavernosus (LA/BC) and hind-limb muscles of WT, AR113Q, and castrated AR113Q males. Nuclei were stained with DAPI. (**B**–**D**) Relative *CLCN1* (**B** and **C**) and *SCN4A* (**D** and **E**) mRNA expression levels in levator ani/bulbocavernosus (**B** and **D**) and hind-limb (**C** and **E**) muscles of WT ($n = 8$), AR113Q ($n = 9$), and castrated WT males ($n = 6$) at 3–5 months and castrated AR113Q males at 18 months ($n = 4$). Data are reported as mean ± SD relative to expression of 18s rRNA. Differences between WT and AR113Q are significant different in hind-limb ($P < 0.01$ for *CLCN1*) and levator ani/bulbocavernosus muscles ($P < 0.001$ for *CLCN1* and *SCN4A*) as determined by ANOVA with the Neuman-Keuls multiple comparison test. SCN4A levels in hind-limb muscle are not significantly different.

immunoreactive intranuclear inclusions, increased expression of *myogenin* and *acetylcholine receptor α-subunit* mRNAs, and electrophysiological evidence of abnormal spontaneous and insertional activity was evident in males by 3–5 months. In contrast, spinal cord pathology was detectable only in mutant males at 24 months and was characterized by AR immunoreactive intranuclear inclusions. We interpret this temporal course of pathology to indicate that disease is initially characterized by myopathic effects in skeletal muscle combined with either functional denervation or distal axonopathy that is reflective of motor neuron dysfunction. Loss of lower motor neurons and spinal cord gliosis are late manifestations of this progressive disorder. Similarly, transgenic mouse models of Kennedy disease have demonstrated functional defects without marked spinal cord pathology (5, 14), supporting the conclusion that motor neuron loss is a late manifestation of Kennedy disease.

The myopathic component of the disease process is readily detectable in AR113Q males and suggests that muscle pathology significantly contributes to the phenotype. We propose that nonsustained myotonia in the levator ani/bulbocavernosus muscles is indicative of altered muscle membrane excitability in the lower urinary tract of AR113Q males and that this leads to functional urinary tract obstruction and death. While similar, though less pronounced, myotonic discharges were observed in hind-limb muscle of AR113Q males, we did not detect behavioral evidence of myotonia in the limbs of these mice, suggesting that this electrophysiological change was not clinically significant. AR113Q mice have a glutamine tract that is longer than that occurring in Kennedy disease patients, where CAG repeat expansions only up to the mid-sixties have been observed (2). Since CAG repeat length correlates inversely with age of onset and disease severity (49), the longer tract in AR113Q males may lead to a more severe phenotype that is evident at an early age.

Muscle pathology may contribute to the Kennedy disease phenotype through both cell autonomous and nonautonomous mechanisms. Emerging evidence in several neurodegenerative disease model systems has revealed important contributions to the disease phenotype by non–cell autonomous pathways of toxicity. A recent study of a conditional mouse model of Huntington disease that overexpressed mutant *huntingtin* exon 1 in certain neuronal populations suggested that pathologic cell interactions were critical for the development of cortical neuronal pathology (50). Similar data have been derived from the study of familial amyotrophic lateral sclerosis resulting from mutations in Cu/Zn superoxide dismutase (SOD1). Results of studies in several transgenic mouse models have demonstrated that the mutant SOD1 protein acting within nonneuronal cells is toxic to motor neurons (51), including microglia (52). These results help to explain why neuron-specific transgenic expression of mutant SOD1 was insufficient to induce motor neuron degeneration in mice (53, 54). Future studies using model systems that express full-length mutant proteins at endogenous levels in a cell-specific manner will help resolve this issue definitively.

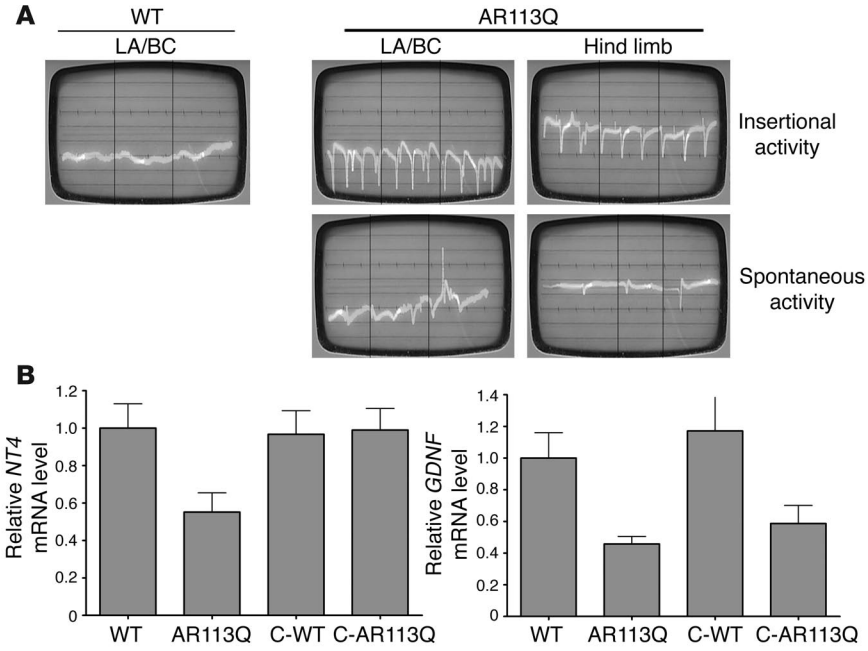

Figure 7
Electrophysiologic and gene expression changes demonstrate myopathy in AR113Q males. (**A**) Composite images from sequential video frames of needle electromyography on levator ani/bulbocavernosus and hind-limb muscles from WT and AR113Q males at 3–5 months. Abnormal spontaneous and insertional activities were observed in both muscle groups of AR113Q males, as indicated by positive, downward deflections of the tracing, but not in WT males. Each horizontal division is equal to 10 ms. (**B**) Relative *NT-4* and *GDNF* mRNA expression levels in hind-limb muscle, determined as in Figure 6. Differences between WT and AR113Q are significant at $P < 0.05$.

These data indicate that pathologic cell interactions play a significant role in the disease phenotype in diverse models of neurodegenerative disorders characterized by protein aggregation. The myopathic effects demonstrated here suggest that similar mechanisms contribute to the progression of Kennedy disease. AR113Q hind-limb muscle expressed significantly lower levels of mRNAs encoding the neurotrophic factors NT-4 and GDNF, indicating that a loss of trophic support from the diseased muscle may hasten lower motor neuron dysfunction and degeneration. That muscle-derived neurotrophic factors can modulate the progression of motor neuron disease was demonstrated by enhanced motor neuron survival in SOD1 mutant mice mediated by transgenic expression of IGF-1 in muscle (55). Our data indicate that myopathic processes may contribute to the progression of Kennedy disease and that skeletal muscle may be a therapeutic target for treating patients with this disorder.

Methods

Mouse strains. Derivation of mice with targeted *Ar* alleles containing 21, 48, or 113 CAG repeats in exon 1 was described previously (27, 28). Reanalysis of the targeting vector used to generate AR48Q mice (previously identified as AR41Q) revealed the presence of 48 rather than 41 CAG repeats. Mice were generated by recombining a portion of human exon 1 encompassing amino acids 31–484 with the mouse *Ar* gene in CJ7 embryonic stem cells. Male chimeras were mated with C57BL/6J females, and females heterozygous for the targeted *Ar* allele were bred with WT C57BL/6J males to generate the N2 and N5 mice used in this study. All procedures involving mice were approved by the University of Michigan Committee on Use and Care of Animals, in accord with the NIH Guidelines for the Care and Use of Experimental Animals.

Hormone manipulation. Male mice underwent orchiectomy at 5–6 weeks of age. Following induction of isoflurane anesthesia, the abdomen was cleaned and shaved, and a 1-cm incision was made at the levels of the legs. The vas deferens and spermatic cord were visualized and ligated with absorbable suture material, the testes removed, and the incision closed with surgical glue.

Pellets containing 12.5 mg testosterone or vehicle control designed for 90-day release were obtained from Innovative Research of America. These pellets were implanted subcutaneously on the dorsal surface of the mouse using a trochar.

Grip-strength analysis. Mice were brought to the testing room and allowed to acclimatize for 10 minutes. A Grip Strength Meter (Columbus Instruments) was used to measure forelimb grip strength. The grip strength meter was positioned horizontally, and mice were held by the tail and lowered toward the apparatus. Mice were allowed to grasp the smooth metal triangular pull bar with their forelimbs only and then were pulled backward in the horizontal plane. The force applied to the bar at the moment the grasp was released was recorded as the peak tension (kg). The test was repeated 5 consecutive times within the same session, and the highest value from the 5 trials was recorded as the grip strength for that animal.

Protein expression analysis. Spinal cords from WT and AR113Q male mice were homogenized in RIPA buffer containing cOmplete Protease Inhibitor Cocktail (Roche Diagnostics) and 0.1% β-mercaptoethanol using a motor homogenizer (TH115; OMNI International). Sample lysates were cleared by centrifugation at 15,000 *g* for 5 minutes at 4°C. Anti-AR antibody (N-20; Santa Cruz Biotechnology Inc.) was conjugated to washed protein A/G-agarose beads (SC-2003; Santa Cruz Biotechnology Inc.). A 2-mg sample lysate was precleared by incubation with protein A/G-agarose beads at 4°C for 10 minutes. The supernatant was collected, then mixed with N-20–conjugated agarose beads and gently rocked at 4°C overnight. The beads were washed thoroughly with ice-cold PBS, resuspended in 2× sample buffer, and boiled for 5 minutes. Samples were resolved by 10% SDS-PAGE and transferred to nitrocellulose membranes (Bio-Rad); proteins were visualized by chemiluminescence (PerkinElmer).

Immunohistochemistry and immunofluorescence. Tissue was fixed in formalin, embedded in paraffin, sectioned at 5 μm, and stained with H&E. For immunohistochemistry on fixed tissue, antigen retrieval was achieved by pretreatment with formic acid for 10 minutes, then boiling in glycine buffer (pH 3.5) for 10 minutes. Tissue sections were stained with antibodies against AR (Santa Cruz Biotechnology Inc.) or expanded glutamine tracts (1C2; Chemicon International). Proteins were visualized using the VECTASTAIN ABC Kit (Vector Laboratories). Light images were captured using an Olympus BX41 Microscope, ×40 lens, and a SPOT Insight digital camera (Diagnostic Instruments). For visualization of CLCN1, 10 μM frozen sections were stained with

a CLCN1-specific antibody (Alpha Diagnostic International) and an Alexa Fluor 594 secondary antibody (Invitrogen). Confocal images were captured using a Zeiss LSM 510 microscope and a water immersion lens (×63).

Gene expression analysis. Total RNA isolated from tissues with TRIzol (Invitrogen) served as a template for cDNA synthesis using the High Capacity cDNA Archive Kit from Applied Biosystems. Gene-specific primers and probes labeled with a fluorescent reporter dye and quencher were purchased from Applied Biosystems. TaqMan assays were performed using 5 ng aliquots of cDNA. Replicate tubes were analyzed for the expression of 18s ribosomal RNA (rRNA) using a VIC-labeled probe. Threshold cycle (Ct) values were determined by an ABI Prism 7900HT Sequence Detection System, and relative expression levels were calculated using the standard curve method of analysis.

Measurement of serum testosterone. Serum testosterone levels were determined by radioimmunoassay (Diagnostic Systems Laboratories) that had a sensitivity of 0.05 ng/ml. The reference preparation of testosterone, obtained from Steraloids Inc., was purified by HPLC and was verified by thin-layer chromatography and immunoassay.

Electromyography. Mice were anesthetized with isoflurane, and levator ani/bulbocavernosus and hind-limb muscles were surgically exposed. Insertional and spontaneous electromyography measurements were taken from each muscle with a 30-gauge concentric needle electrode (25 mm × 0.30 mm). Needle advancements were made in at least 4 directions for each muscle. Duration of insertional activity was measured in increments of 100 ms (10 ms/div) with gain set at 50 μV per interval. Low- and high-pass filter settings were 2 Hz and 10 kHz, respectively. Needle electromyography data were collected and analyzed with a Teca TD-20 unit (Teca Corp.) and recorded with a digital video camera.

Statistics. Statistical significance was assessed using a 2-tailed Student's *t* test or ANOVA with the Newman-Keuls multiple comparison test, as determined using the software package Prism 4 (GraphPad Software). *P* values less than 0.05 were considered significant.

Acknowledgments

We thank S. Marc Breedlove and Maurice Swanson for helpful discussions, the University of Michigan Transgenic Animal Core and the Microscopy and Image Analysis Laboratory for assistance with this project, and Elizabeth Walker for preparation of the figures. This work was supported by a Beeson Career Development Award from the NIH and American Federation for Aging Research (K08 AG024758 to A.P. Lieberman), and by grants from the NIH (NS045195 to C. Jordan), the Department of Defense (DAMD17-02-1-0099 to D.M. Robbins), the Muscular Dystrophy Association (3393 to A.P. Lieberman), the Kennedy's Disease Association (to A.P. Lieberman), and the University of Michigan Nathan Shock Center Rodent Core and Biomedical Research Council (to A.P. Lieberman).

Received for publication April 7, 2006, and accepted in revised form July 25, 2006.

Address correspondence to: Andrew Lieberman, Department of Pathology, University of Michigan Medical School, 3510 MSRB 1, 1150 West Medical Center Drive, Ann Arbor, Michigan 48109-0605, USA. Phone: (734) 936-1887; Fax: (734) 615-3441; E-mail: liebermn@umich.edu.

1. Zoghbi, H.Y., and Orr, H.T. 2000. Glutamine repeats and neurode generation. *Annu. Rev. Neurosci.* **23**:217–247.
2. Lieberman, A.P., and Fischbeck, K.H. 2000. Triplet repeat expansion in neuromuscular disease. *Muscle Nerve.* **23**:843–850.
3. Katsuno, M., et al. 2006. Pathogenesis, animal models and therapeutics in Spinal and bulbar muscular atrophy (SBMA). *Exp. Neurol.* **200**:8–18.
4. Sperfeld, A.D., et al. 2002. X-linked bulbospinal neuronopathy: Kennedy disease. *Arch. Neurol.* **59**:1921–1926.
5. Abel, A., Walcott, J., Woods, J., Duda, J., and Merry, D.E. 2001. Expression of expanded repeat androgen receptor produces neurologic disease in transgenic mice. *Hum. Mol. Genet.* **10**:107–116.
6. Merry, D.E., Kobayashi, Y., Bailey, C.K., Taye, A.A., and Fischbeck, K.H. 1998. Cleavage, aggregation and toxicity of the expanded androgen receptor in spinal and bulbar muscular atrophy. *Hum. Mol. Genet.* **7**:693–701.
7. Thomas, M., et al. 2005. The unfolded protein response modulates toxicity of the expanded glutamine androgen receptor. *J. Biol. Chem.* **280**:21264–21271.
8. Piccioni, F., et al. 2002. Androgen receptor with elongated polyglutamine tract forms aggregates that alter axonal trafficking and mitochondrial distribution in motor neuronal processes. *FASEB J.* **16**:1418–1420.
9. Szebenyi, G., et al. 2003. Neuropathogenic forms of huntingtin and androgen receptor inhibit fast axonal transport. *Neuron.* **40**:41–52.
10. Morfini, G., et al. 2006. JNK mediates pathogenic effects of polyglutamine-expanded androgen receptor on fast axonal transport. *Nat. Neurosci.* **9**:907–916.
11. McCampbell, A., et al. 2001. Histone deacetylase inhibitors reduce polyglutamine toxicity. *Proc. Natl. Acad. Sci. U. S. A.* **98**:15179–15184.
12. McCampbell, A., et al. 2000. CREB-binding protein sequestration by expanded polyglutamine. *Hum. Mol. Genet.* **9**:2197–2202.
13. McManamny, P., et al. 2002. A mouse model of spinal and bulbar muscular atrophy. *Hum. Mol. Genet.* **11**:2103–2111.
14. Chevalier-Larsen, E.S., et al. 2004. Castration restores function and neurofilament alterations of aged symptomatic males in a transgenic mouse model of spinal and bulbar muscular atrophy. *J. Neurosci.* **24**:4778–4786.
15. Katsuno, M., et al. 2002. Testosterone reduction prevents phenotypic expression in a transgenic mouse model of spinal and bulbar muscular atrophy. *Neuron.* **35**:843–854.
16. Sopher, B.L., et al. 2004. Androgen receptor YAC transgenic mice recapitulate SBMA motor neuronopathy and implicate VEGF164 in the motor neuron degeneration. *Neuron.* **41**:687–699.
17. Thomas, M., et al. 2004. Androgen receptor acetylation site mutations cause trafficking defects, misfolding, and aggregation similar to expanded glutamine tracts. *J. Biol. Chem.* **279**:8389–8395.
18. Thomas, M., et al. 2006. Pharmacologic and genetic inhibition of hsp90-dependent trafficking reduces aggregation and promotes degradation of the expanded glutamine androgen receptor without stress protein induction. *Hum. Mol. Genet.* **15**:1876–1883.
19. Sobue, G., et al. 1993. Subclinical phenotypic expressions in heterozygous females of X-linked recessive bulbospinal neuronopathy. *J. Neurol. Sci.* **117**:74–78.
20. Schmidt, B.J., Greenberg, C.R., Allingham-Hawkins, D.J., and Spriggs, E.L. 2002. Expression of X-linked bulbospinal muscular atrophy (Kennedy disease) in two homozygous women. *Neurology.* **59**:770–772.
21. Katsuno, M., et al. 2003. Leuprorelin rescues polyglutamine-dependent phenotypes in a transgenic mouse model of spinal and bulbar muscular atrophy. *Nat. Med.* **9**:768–773.
22. Kazemi-Esfarjani, P., Trifiro, M.A., and Pinsky, L. 1995. Evidence for a repressive function of the long polyglutamine tract in the human androgen receptor: possible pathogenetic relevance for the (CAG)n-expanded neuronopathies. *Hum. Mol. Genet.* **4**:523–527.
23. Lieberman, A.P., Harmison, G., Strand, A.D., Olson, J.M., and Fischbeck, K.H. 2002. Altered transcriptional regulation in cells expressing the expanded polyglutamine androgen receptor. *Hum. Mol. Genet.* **11**:1967–1976.
24. Mhatre, A.N., et al. 1993. Reduced transcriptional regulatory competence of the androgen receptor in X-linked spinal and bulbar muscular atrophy. *Nat. Genet.* **5**:184–188.
25. Chamberlain, N.L., Driver, E.D., and Miesfeld, R.L. 1994. The length and location of CAG trinucleotide repeats in the androgen receptor N-terminal domain affect transactivation function. *Nucleic Acids Res.* **22**:3181–3186.
26. Fischbeck, K.H., Lieberman, A., Bailey, C.K., Abel, A., and Merry, D.E. 1999. Androgen receptor mutation in Kennedy's disease. *Philos. Trans. R. Soc. Lond. B. Biol. Sci.* **354**:1075–1078.
27. Yu, Z., et al. 2006. Abnormalities of germ cell maturation and sertoli cell cytoskeleton in androgen receptor 113 CAG knock-in mice reveal toxic effects of the mutant protein. *Am. J. Pathol.* **168**:195–204.
28. Albertelli, M.A., Scheller, A., Brogley, M., and Robins, D.M. 2006. Replacing the mouse androgen receptor with human alleles demonstrates glutamine tract length dependent effects on physiology and tumorigenesis in mice. *Mol. Endocrinol.* **20**:1248–1260.
29. Kennedy, W.R., Alter, M., and Sung, J.H. 1968. Progressive proximal spinal and bulbar muscular atrophy of late onset. A sex-linked recessive trait. *Neurology.* **18**:671–680.
30. Sobue, G., et al. 1989. X-linked recessive bulbospinal neuronopathy. A clinicopathological study. *Brain.* **112**:209–232.
31. Klocke, R., Steinmeyer, K., Jentsch, T.J., and Jockusch, H.

1994. Role of innervation, excitability, and myogenic factors in the expression of the muscular chloride channel ClC-1. A study on normal and myotonic muscle. *J. Biol. Chem.* **269**:27635–27639.
32. Kostrominova, T.Y., Dow, D.E., Dennis, R.G., Miller, R.A., and Faulkner, J.A. 2005. Comparison of gene expression of 2-mo denervated, 2-mo stimulated-denervated, and control rat skeletal muscles. *Physiol. Genomics.* **22**:227–243.
33. Mejat, A., et al. 2005. Histone deacetylase 9 couples neuronal activity to muscle chromatin acetylation and gene expression. *Nat. Neurosci.* **8**:313–321.
34. Strand, A.D., et al. 2005. Gene expression in Huntington's disease skeletal muscle: a potential biomarker. *Hum. Mol. Genet.* **14**:1863–1876.
35. Tullis, K.M., Krebs, C.J., Leung, J.Y., and Robins, D.M. 2003. The regulator of sex-limitation gene, rsl, enforces male-specific liver gene expression by negative regulation. *Endocrinology.* **144**:1854–1860.
36. Schroder, H.D. 1980. Organization of the motoneurons innervating the pelvic muscles of the male rat. *J. Comp. Neurol.* **192**:567–587.
37. Forger, N.G., Hodges, L.L., Roberts, S.L., and Breedlove, S.M. 1992. Regulation of motoneuron death in the spinal nucleus of the bulbocavernosus. *J. Neurobiol.* **23**:1192–1203.
38. Forger, N.G., Roberts, S.L., Wong, V., and Breedlove, S.M. 1993. Ciliary neurotrophic factor maintains motoneurons and their target muscles in developing rats. *J. Neurosci.* **13**:4720–4726.
39. Xu, J., Gingras, K.M., Bengston, L., Di Marco, A., and Forger, N.G. 2001. Blockade of endogenous neurotrophic factors prevents the androgenic rescue of rat spinal motoneurons. *J. Neurosci.* **21**:4366–4372.
40. Jordan, C.L., Breedlove, S.M., and Arnold, A.P. 1991. Ontogeny of steroid accumulation in spinal lumbar motoneurons of the rat: implications for androgen's site of action during synapse elimination. *J. Comp. Neurol.* **313**:441–448.
41. Jordan, C.L., Padgett, B., Hershey, J., Prins, G., and Arnold, A. 1997. Ontogeny of androgen receptor immunoreactivity in lumbar motoneurons and in the sexually dimorphic levator ani muscle of male rats. *J. Comp. Neurol.* **379**:88–98.
42. Monks, D.A., O'Bryant, E.L., and Jordan, C.L. 2004. Androgen receptor immunoreactivity in skeletal muscle: enrichment at the neuromuscular junction. *J. Comp. Neurol.* **473**:59–72.
43. Koch, M.C., et al. 1992. The skeletal muscle chloride channel in dominant and recessive human myotonia. *Science.* **257**:797–800.
44. Charlet, B.N., et al. 2002. Loss of the muscle-specific chloride channel in type 1 myotonic dystrophy due to misregulated alternative splicing. *Mol. Cell.* **10**:45–53.
45. Mankodi, A., et al. 2002. Expanded CUG repeats trigger aberrant splicing of ClC-1 chloride channel pre-mRNA and hyperexcitability of skeletal muscle in myotonic dystrophy. *Mol. Cell.* **10**:35–44.
46. Kanadia, R.N., et al. 2003. A muscleblind knockout model for myotonic dystrophy. *Science.* **302**:1978–1980.
47. England, J.D. 2001. Mutant sodium channels, myotonia, and propofol. *Muscle Nerve.* **24**:713–715.
48. Sendtner, M., Pei, G., Beck, M., Schweizer, U., and Wiese, S. 2000. Developmental motoneuron cell death and neurotrophic factors. *Cell Tissue Res.* **301**:71–84.
49. La Spada, A.R., et al. 1992. Meiotic stability and genotype-phenotype correlation of the trinucleotide repeat in X-linked spinal and bulbar muscular atrophy. *Nat. Genet.* **2**:301–304.
50. Gu, X., et al. 2005. Pathological cell-cell interactions elicited by a neuropathogenic form of mutant Huntingtin contribute to cortical pathogenesis in HD mice. *Neuron.* **46**:433–444.
51. Clement, A.M., et al. 2003. Wild-type nonneuronal cells extend survival of SOD1 mutant motor neurons in ALS mice. *Science.* **302**:113–117.
52. Boillee, S., et al. 2006. Onset and progression in inherited ALS determined by motor neurons and microglia. *Science.* **312**:1389–1392.
53. Lino, M.M., Schneider, C., and Caroni, P. 2002. Accumulation of SOD1 mutants in postnatal motoneurons does not cause motoneuron pathology or motoneuron disease. *J. Neurosci.* **22**:4825–4832.
54. Pramatarova, A., Laganiere, J., Roussel, J., Brisebois, K., and Rouleau, G.A. 2001. Neuron-specific expression of mutant superoxide dismutase 1 in transgenic mice does not lead to motor impairment. *J. Neurosci.* **21**:3369–3374.
55. Dobrowolny, G., et al. 2005. Muscle expression of a local Igf-1 isoform protects motor neurons in an ALS mouse model. *J. Cell Biol.* **168**:193–199.